Lab on a Chip

Miniaturisation for chemistry, physics, biology, & bioengineering

www.rsc.org/loc

Volume 9 | Number 13 | 7 July 2009 | Pages 1817–1972

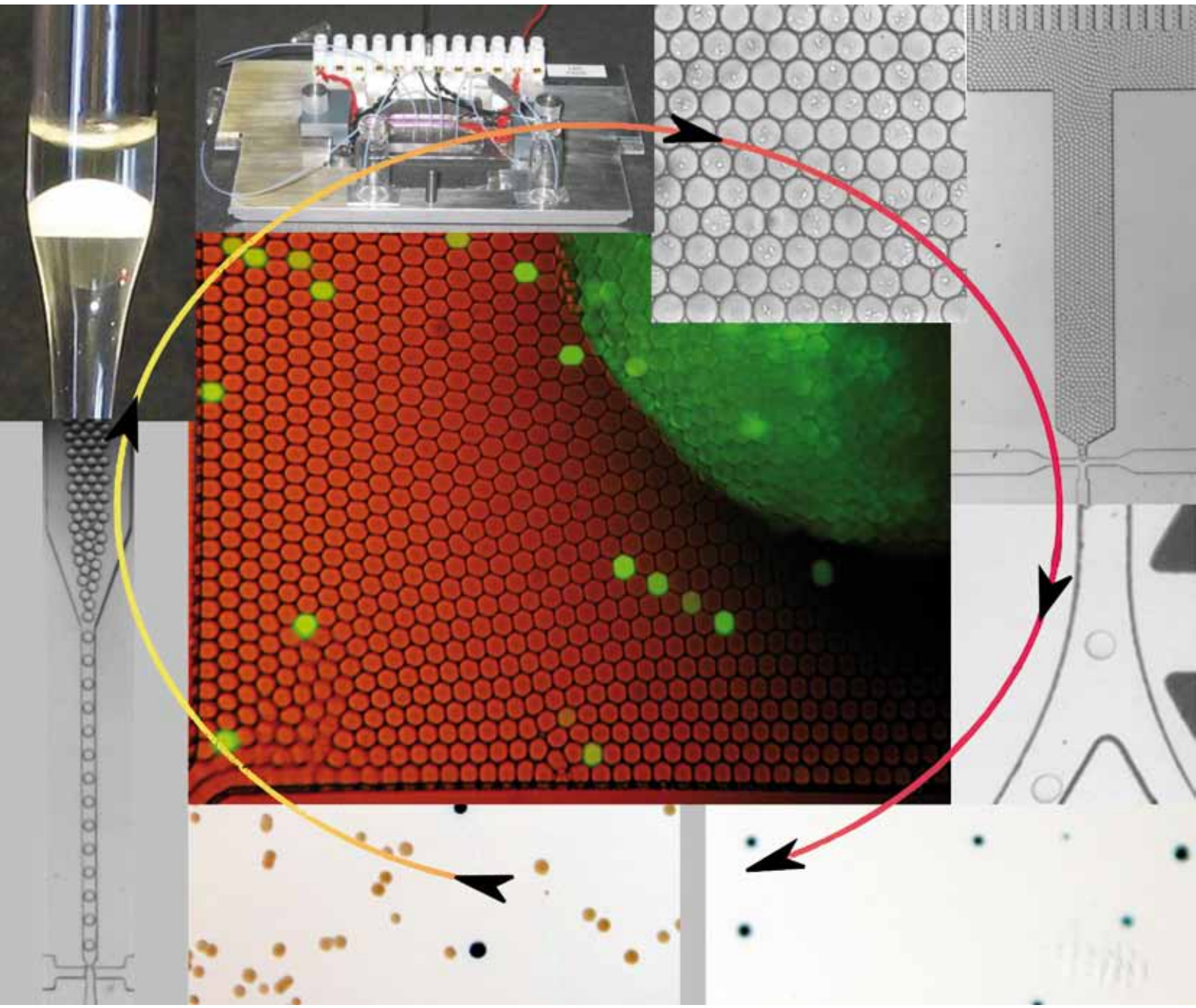

ISSN 1473-0197

RSC Publishing

Fluorescence-activated droplet sorting (FADS): efficient microfluidic cell sorting based on enzymatic activity†

Jean-Christophe Baret,‡[a] Oliver J. Miller,‡[a] Valerie Taly,[a] Michaël Ryckelynck,[a] Abdeslam El-Harrak,[a] Lucas Frenz,[a] Christian Rick,[a] Michael L. Samuels,[b] J. Brian Hutchison,[b] Jeremy J. Agresti,[c] Darren R. Link,[b] David A. Weitz[c] and Andrew D. Griffiths*[a]

Received 5th February 2009, Accepted 14th April 2009
First published as an Advance Article on the web 23rd April 2009
DOI: 10.1039/b902504a

We describe a highly efficient microfluidic fluorescence-activated droplet sorter (FADS) combining many of the advantages of microtitre-plate screening and traditional fluorescence-activated cell sorting (FACS). Single cells are compartmentalized in emulsion droplets, which can be sorted using dielectrophoresis in a fluorescence-activated manner (as in FACS) at rates up to 2000 droplets s^{-1}. To validate the system, mixtures of *E. coli* cells, expressing either the reporter enzyme β-galactosidase or an inactive variant, were compartmentalized with a fluorogenic substrate and sorted at rates of ~300 droplets s^{-1}. The false positive error rate of the sorter at this throughput was <1 in 10^4 droplets. Analysis of the sorted cells revealed that the primary limit to enrichment was the co-encapsulation of *E. coli* cells, not sorting errors: a theoretical model based on the Poisson distribution accurately predicted the observed enrichment values using the starting cell density (cells per droplet) and the ratio of active to inactive cells. When the cells were encapsulated at low density (~1 cell for every 50 droplets), sorting was very efficient and all of the recovered cells were the active strain. In addition, single active droplets were sorted and cells were successfully recovered.

Introduction

The compartmentalization of assays in wells makes microtitre-plates the most flexible and most widely used screening platform in use today. However, reducing assay volumes to below 1–2 μl is problematic[1] and the maximum throughput, even when using sophisticated (and expensive) robotic handling, is little more than 1 s^{-1}. In contrast, fluorescence-activated cell sorting (FACS) is capable of analyzing and sorting cells at a rate of up to 7×10^4 cells s^{-1}.[2] However, during FACS, cell fluorescence is detected in a continuous aqueous stream[3] and the absence of compartmentalization limits the range of activities that can be screened: the fluorescent marker(s) must remain either inside or on the surface of the cells to be sorted. This makes detection of secreted enzymes using fluorogenic substrates impossible. Additionally, if the enzyme is intracellular, then the cell may be impermeable to the substrate or the product may freely diffuse out of the cell. Conventional FACS machines also require typically more than 10^5 cells in the starting population,[3] are very expensive and generate aerosols with serious biosafety ramifications.[4]

Microfluidic flow sorting systems have the potential to offer solutions to these problems, enabling the handling of small numbers of cells in inexpensive, sterile, aerosol-free, disposable devices.[2,5] Several approaches have already been demonstrated, including devices that sort cells by dielectrophoretic actuation, electrokinetic actuation, hydrodynamic flow-switching and optical forces (listed by Perroud *et al.*).[6] However, as with conventional FACS, the absence of assay compartmentalization limits their flexibility.

The versatility of conventional FACS can be increased by *in vitro* compartmentalization (IVC)[7] of assays in emulsion droplets, allowing selection for enzymatic activity.[8,9] However, the technique has three main limitations: complex double emulsions structures must be generated; the emulsions are highly polydisperse, limiting quantitative analysis; and the capacity to modify the contents of droplets after encapsulation is restricted.[10] These limitations can, however, be overcome by using droplet-based microfluidic systems, which allow the generation of highly monodisperse emulsions[11] and the fusion[12–14] and splitting[12,15,16] of droplets. It has even been possible to separate or sort droplets by charging them and steering them with an electric field[17] or by exploiting dielectrophoresis,[18] electrocoalescence,[19] localized heating,[20] or Rayleigh–Plateau instabilities.[21] It has not, however, been possible to selectively enrich specific subpopulations of droplets according to their fluorescence until now.

This manuscript describes a highly efficient droplet-based microfluidic FACS, optimized to sort picolitre-range droplets by dielectrophoresis.[17,18] This fluorescence-activated droplet sorting (FADS) system combines many of the advantages of microtitre-plate screening and fluorescence-activated cell sorting (FACS): assays are compartmentalized in emulsion droplets, which are the functional equivalent of microtitre-plate wells, but can be analyzed and sorted at high speed (as in FACS). Although several techniques for monitoring fluorescent reactions[22,23] and

[a]*Institut de Science et d'Ingénierie Supramoléculaires (ISIS), Université de Strasbourg, CNRS UMR 7006, 8 allée Gaspard Monge, BP 70028, F-67083 Strasbourg Cedex, France. E-mail: griffiths@isis.u-strasbg.fr.*
[b]*RainDance Technologies, Inc., 44 Hartwell Avenue, Lexington, MA, 02421, USA*
[c]*Department of Physics and School of Engineering and Applied Sciences, Harvard University, Cambridge, USA*

† Electronic supplementary information (ESI) available: Model for cellular enrichment by FADS, supplementary Fig. S1–8, Table 1 and Movies S1–6. See DOI: 10.1039/b902504a

‡ These two authors contributed to the work equally.

fluorescent cells[24] in droplets have already been described, we report the first system capable of actually sorting droplets according to their fluorescence. This microfluidic system is also the first to be capable of sorting cells according to enzymatic activity. This latter application involves the following steps: (i) encapsulating a mixed population of cells in the droplets of a biocompatible emulsion; (ii) storing the emulsion to allow time for the fluorogenic substrate in each droplet to be turned-over by a cellular enzyme (if present); (iii) sorting the droplets according to fluorescence intensity (substrate turn-over) in a microfluidic sorting device; and (iv) recovering the cells from the sorted droplets. Such facile enrichment of specific cells according to enzymatic activity should provide a boon to fields such as directed evolution, where large libraries are functionally screened.

Results and discussion

Factors affecting sorting

12 pl monodisperse droplets containing 250 μM fluorescein were generated by the microfluidic flow-focusing of an aqueous stream by twin streams of fluorinated oil containing a surfactant[11] (Fig. 1a and Movie S1 in the ESI).† The surfactant-stabilized droplets were collected in a reservoir (Fig. 1b) and subsequently injected into the microfluidic sorting device where they were spaced-out (Fig. 1c and Movie S2 in the ESI)† and sorted at an asymmetric Y-shaped junction (Fig. 1d). The fluorescence of each droplet was measured with a photomultiplier tube (PMT) as it passed through a 488 nm laser line (Fig. 2). Droplets flowed down the wider 'negative' arm of the sorting junction by default due to its lower hydraulic resistance (Fig. 1d). If a particular droplet was chosen for sorting then a pulse of high-voltage alternating current (AC) was applied across the electrodes adjacent to the sorting junction. The resulting electric field deflected the droplet of interest into the narrower 'positive' arm of the junction by dielectrophoresis (Fig. 1d).

The frequency of droplet reinjection was found to correlate with the flow rate of reinjection in a linear fashion, as expected

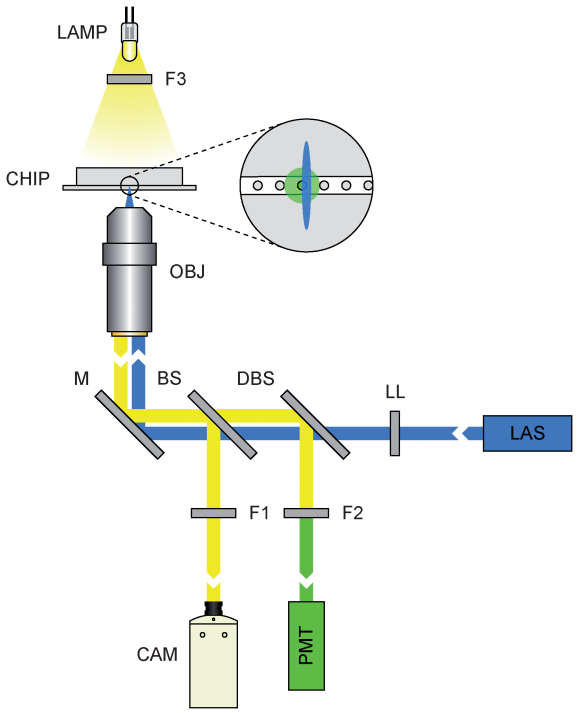

Fig. 2 Schematic representation of the optical setup. Laser light (488 nm) was emitted from the laser (LAS), shaped into a laser line (LL) and transmitted through a multi-edge dichroic beam splitter (DBS) to the microscope. Inside the microscope the laser light passed through a beam splitter (BS) and was reflected up into the objective by a conventional mirror (M). The shaped laser beam was focused to a ~10 × ~150 μm line across the sorting channel in the microfluidic chip (CHIP) where it excited droplets one at a time as they flowed past. The fluorescent emission from each droplet passed back along the path of the laser beam, but was reflected by the dichroic beam splitter (DBS) to the sensor of the photomultiplier tube (PMT) *via* a bandpass filter (F2). Filtered light from the microscope's halogen lamp (LAMP) illuminated the channels and droplets, allowing the trajectories of droplets to be monitored by the high-speed camera (CAM). The filter F3 removed wavelengths of light that were detected by the PMT to avoid a high background signal.

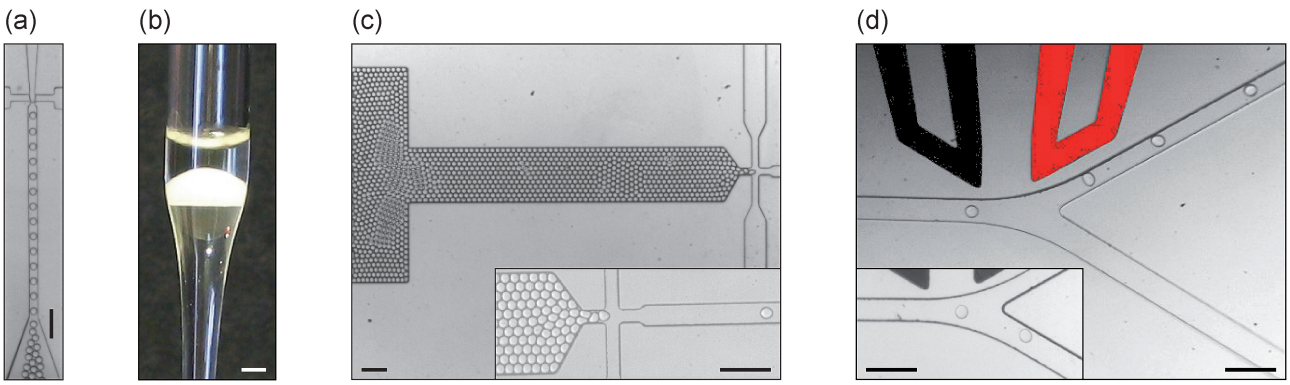

Fig. 1 Generating and sorting droplets triggered on droplet fluorescence. (a) Generation of a monodisperse emulsion by a microfluidic droplet production device. 12 pl aqueous droplets were generated in fluorinated oil containing surfactant by flow-focusing (Movie S1, ESI).†(b) Droplets being incubated in a Pasteur pipette. The droplets have floated up to the interface between the fluorinated oil and a layer of LB above. (c) Reinjection of a monodisperse emulsion into the sorting device (Movie S2, ESI).† The inset image shows the emulsion droplets being spaced-out with surfactant-free fluorinated oil. (d) Trajectories of droplets stream through the sorting junction. When an AC electric field was applied across the electrodes (1–1.4 $kV_{p\text{-}p}$), the droplets were deflected into the positive arm (Movie S3).† In the absence of a field, the droplets flowed into the negative arm owing to the lower hydraulic resistance (inset). The length of the scale-bar in each photograph is 100 μm, except in (b) where it is 1 mm.

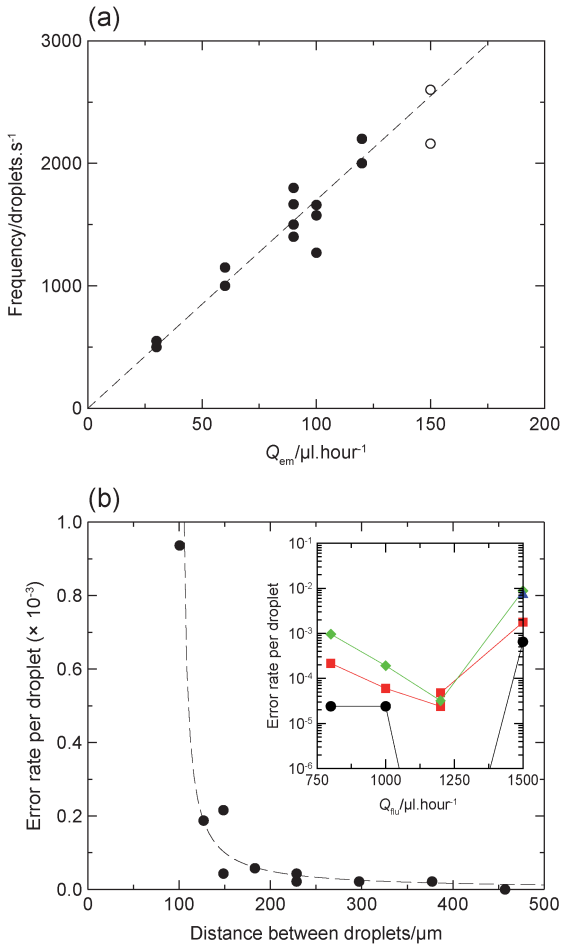

Fig. 3 Limits to the reinjection of 12 pl droplets. (a) The frequency of droplet reinjection was determined solely by the flow rate of the emulsion and was independent of the flow rate of the fluorinated oil. Open circles indicate data points where droplet-breakup was observed. (b) False positive error rate. The flow rate of the fluorinated oil determined the false positive error rate when the droplet reinjection rate was fixed. The lowest error rates were observed when the flow rate of the fluorinated oil was in the range 1–1.25 ml h^{-1}, with no errors at all observed over 1 min at a reinjection rate of ~500 droplets s^{-1} (inset). The black circles correspond to an emulsion reinjection rate of 30 µl h^{-1} (~500 droplets s^{-1}), the red squares to 60 µl h^{-1} (~1000 droplets s^{-1}), the green diamonds to 90 µl h^{-1} (~1500 droplets s^{-1}) and the blue triangle to 120 µl h^{-1} (~2000 droplets s^{-1}). The fluorinated oil flow rate controlled the spacing of the droplets and sufficient droplet spacing (>200 µm) minimized the false positive error rate (main graph; the dashed line is a guide for the eye; data for all four reinjection rates are combined, excluding cases where droplet-breakup was observed).

(Fig. 3a). The maximum reinjection rate achieved was 2000 droplets s^{-1}: higher reinjection rates resulted in shearing of the droplets into smaller fragments.

The flow rate of the fluorinated oil did not influence the droplet reinjection frequency, but only the distance between two successive droplets with higher flow rates yielding a greater droplet spacing. Flow rates greater than 1.5 ml h^{-1} caused the breakup of 12 pl droplets at the reinjection nozzle, creating pairs of droplets of different sizes. The spacing between droplets was found to be an important factor affecting sorting efficiency. When too close, successive droplets impacted at the sorting junction, causing droplets to flow down the positive arm of the sorting junction in the absence of an electric field ('false positive errors'). False positive error rates were estimated by focusing the laser over the positive arm, counting the number of fluorescent droplets that passed along it over a period of 1 minute and dividing this figure by the number of droplets reinjected per minute. At a given droplet reinjection rate, the false positive error rate was observed to first decrease and then increase again with increasing fluorinated oil flow rate (Fig. 3b). The initial decrease was linked to the increase in droplet spacing, which reduced droplet impacts and favored the correct functioning of the sorter. When correctly spaced, the false positive error rate decreased to below 1 in 10^4 droplets (1–1.25 ml h^{-1} for the fluorinated oil flow rate and <60 µl h^{-1} or <1000 droplets s^{-1} for the emulsion reinjection rate). Increasing the fluorinated oil flow rate further resulted in an increase in the false positive error rate due to droplet breakup and, hence, emulsion polydispersity. However, it is worth noting that the false positive error rate was always less than 1 in 100 droplets under all conditions studied, even at a reinjection rate of 2000 droplets s^{-1}.

We were able to use electric actuation to deflect single droplets at throughputs up to 2000 droplets s^{-1}. Above this rate, it was not possible to reliably deflect every droplet. Two parameters were found to affect the deflection of droplets by dielectrophoresis: the intensity of the electric field and the time over which it was applied. We found that the field needed to be applied for at least 0.5 ms to successfully pull the droplet into the positive arm of the junction. This fact placed an upper limit on the rate of sorting of 2000 droplets s^{-1} (1 s/0.5 ms = 2000). This limit could not be overridden by increasing the voltage across the electrodes; indeed, increasing the voltage above 1.8 $kV_{p\text{-}p}$ caused tip-streaming of the droplets, resulting in depolarization and a much lower sorting efficiency. The optimum was found to be in the range 1.4–1.6 $kV_{p\text{-}p}$, which was effective at deflecting droplets at a reinjection rate of 2000 droplets s^{-1} and at all rates below.

Measurement of sorting efficiency

The false positive and false negative error rates of the asymmetric sorting device (Fig. 1d) were accurately determined by image analysis of droplet trajectories during the sorting of a binary emulsion. False positive errors were defined as negative droplets wrongly entering the positive channel, while false negative errors were defined as positive droplets wrongly entering the negative channel.

A 'dual-emulsifier' device (Fig. S1b and Movie S4, ESI)† was used to generate two types of 12 pl droplet in parallel containing fluorescein at either 25 or 100 µM concentration. The binary emulsion was collected and then injected into the sorting device. Two distinct populations of droplets were observed differing in fluorescence by a factor of four, as expected (Fig. 4a and 4b). A minimum threshold for sorting was set between these two populations and the emulsion was sorted for several hours. High-speed movies recorded during this process were analyzed to determine the error rates of the device (Fig. 4c and 4d and Movie S3 in the ESI).† The false positive and false negative error rates while sorting at 300 droplets s^{-1} were found to be <1 in 10^4 droplets and ~1 in 1000 droplets, respectively.

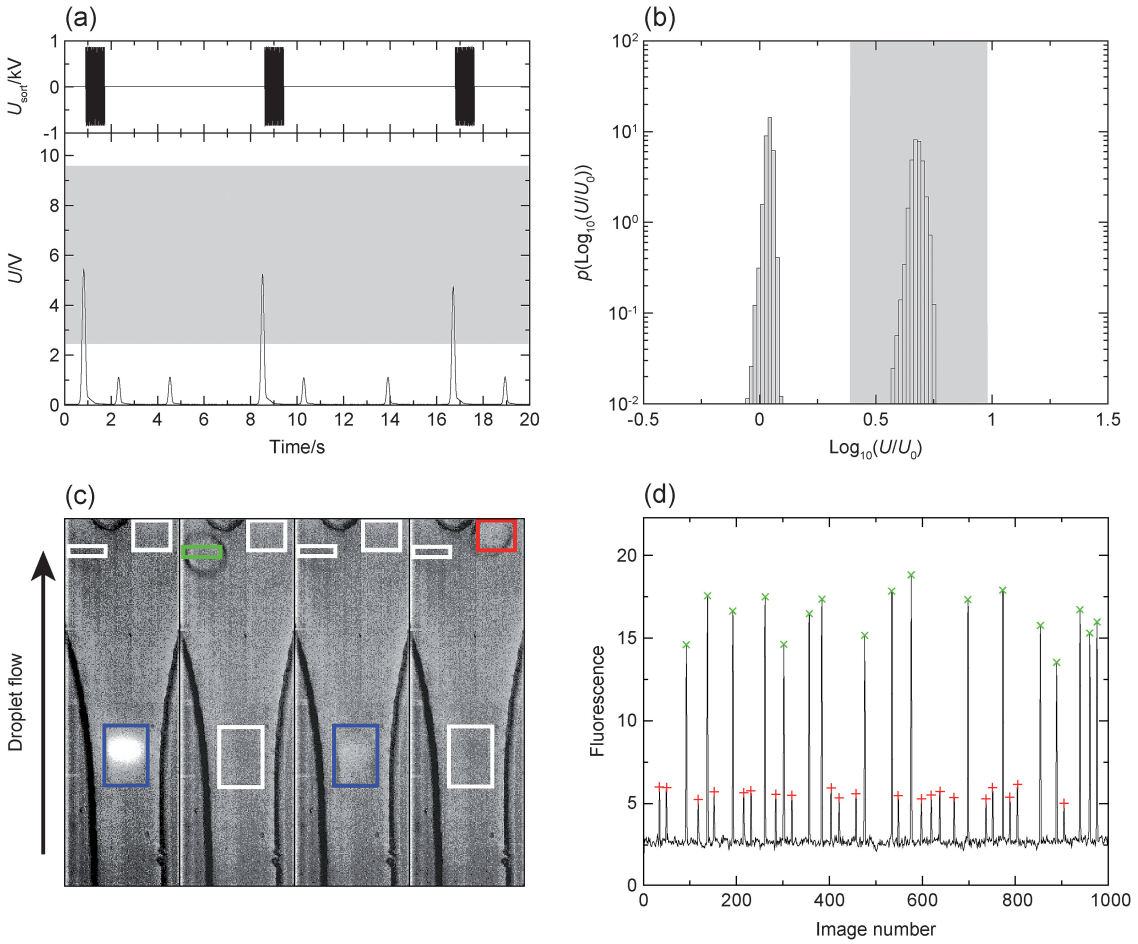

Fig. 4 Measurement of the sorting efficiency. (a) Time sequences of the PMT signal (U; volts) and the AC pulses applied in response to sorting decisions (U_{sort}; volts). The field was applied on the falling edge of fluorescent peaks that exceeded the threshold voltage (in gray). U_0 was a reference voltage (1 V). (b) Histograms of the fluorescent signals in a mixed emulsion containing droplets of 25 and 100 μM sodium fluorescein. The two populations of droplets were clearly separated, with the sorting gate (in gray) selecting only the high-fluorescence droplets. (c) Individual frames from the high-speed camera during sorting of the mixed emulsion, processed by MATLAB. In the first frame, the arrival of a highly fluorescent droplet (100 μM fluorescein) at the junction was observed and its fluorescence was determined (blue box). The trajectory of this droplet through the junction was monitored by examining pixel changes in the two arms (second frame). In this case, the droplet was correctly sorted into the positive arm (green box). In the third frame, a low fluorescence droplet (25 μM fluorescein) arrived at the junction and was registered (blue box). The droplet did not trigger the sorting mechanism and correctly flowed down the negative arm of the junction (red box in fourth frame). (d) A plot of the pixel intensity (fluorescence) at the junction entrance over a period of 20 ms (1000 camera frames collected at a frequency of 5 kHz). To verify sorting events, droplets were classified as containing either 25 or 100 μM fluorescein by virtue of their fluorescence at the mouth of the sorting junction. The subsequent trajectory of each droplet through the junction was tracked: droplets ending up in the positive and negative arms of the junction are depicted in the plot with green and red markers, respectively. Comparing the identity of each droplet with its subsequent trajectory allowed the false positive and the false negative error rates for the sorting device to be determined. In total, 1.3×10^5 images (40 gigabytes) were analyzed, corresponding to 10^4 droplets.

Sorting cells in droplets based on enzymatic activity

To determine the efficiency of the sorting device when sorting cells, we used two strains of *E. coli*: one strain expressing the classic reporter gene *lacZ* (encoding β-galactosidase) and the other expressing an inactive, frameshifted variant, Δ*lacZ*. Mixtures of these cells were emulsified with a fluorogenic β-galactosidase substrate (fluorescein-di-β-D-galactopyranoside; FDG) in 12 pl droplets using a microfluidic device. The emulsions were incubated at 20 °C for 14 hours (Fig. 1b) to allow time for cell growth and substrate hydrolysis by the enzyme. Following incubation, droplets containing *lacZ* cells were 100-fold more fluorescent than either empty droplets or those containing Δ*lacZ* cells (Fig. 5). We sorted the high fluorescence droplets from each emulsion at a rate of 300 droplets s^{-1} (Movie S5, ESI)† and recovered and grew the cells to determine enrichment values.

FACS of live *E. coli* cells is normally precluded by their impermeability to FDG: the integrity of their membranes needs to be compromised for the substrate to come into contact with the cytoplasmic β-galactosidase.[25] However, when *E. coli* cells are compartmentalized in droplets, as here, they can be lyzed *in situ*, for example using polymyxin B.[26] The released β-galactosidase and the fluorescent product (fluorescein) remain in the droplet, allowing identification and, potentially, sorting (Fig. S2, ESI).† Such an approach, however, prevents the recovery of

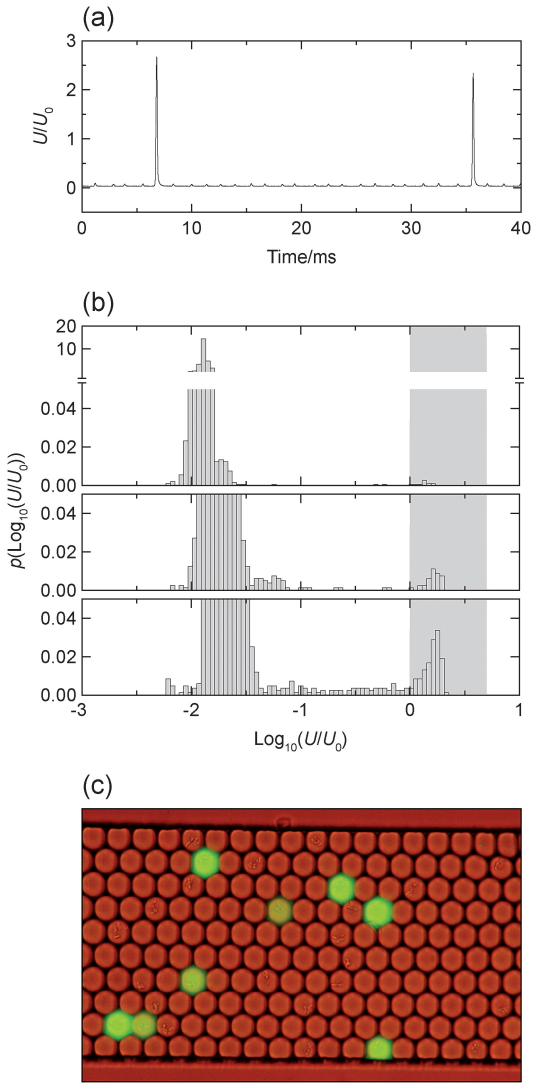

Fig. 5 Detection of β-galactosidase activity in cells in droplets. (a) Time sequence of the fluorescence analysis. Droplets could be analyzed at very high-throughput: up to 10^4 per second. (b) Histograms of the fluorescent signals of droplets in an emulsion containing both *lacZ* and Δ*lacZ* bacteria: ε_0 was 0.1 and λ was either 0.016 (upper graph), 0.16 (middle graph) or 1.6 (lower graph). In each case the two populations of droplets were separated, with the sorting gate (in gray) selecting only the high-fluorescence (*lacZ*) droplets. U was the signal from the PMT (volts) and U_0 was a reference voltage (1 V). (c) Fluorescence micrograph of droplets containing *lacZ* bacteria in the channel of a microfluidic device. Each droplet functioned as an independent microreactor with 10%–20% of the occupied droplets converting the non-fluorescent substrate FDG to fluorescent fluorescein.

viable cells after sorting and necessitates DNA amplification and retransformation steps. To avoid these steps and, thus, simplify the characterization of the sorting device, we used an alternative strategy. We observed, while examining emulsions containing only *lacZ* bacteria, that even in the absence of a lytic agent 10–20% of the occupied droplets were fluorescent (Fig. 5c and Fig. S2a in the ESI),† indicating the presence of one or more lyzed cells in each fluorescent droplet. This allowed us to sort viable *E. coli* based on β-galactosidase activity in a similar manner to Nir *et al.*, who used FACS to sort small colonies of *E. coli* in agarose microbeads in which only a fraction of the cells were lyzed to catalyze FDG cleavage.[25] In both cases, it was the presence of a small clonal population of bacteria in each droplet/microbead that allowed sorting of viable cells: a minority of the population lyzed to expose β-galactosidase activity and the majority remained intact, facilitating recovery (Movie S6, ESI).† Approximately 50 viable cells were recovered per droplet, regardless of the fluorescence.

With the low error rate of the sorting device, the main factor expected to affect enrichment was the co-compartmentalization of Δ*lacZ* cells with *lacZ* cells. We expected the distribution of cells between droplets during encapsulation to follow the Poisson distribution.[22,27,28] A model for enrichment was developed based upon the Poisson distribution (ESI).† In summary, the theoretical enrichment (η_m) is given by the equation:

$$\eta_m = \frac{1}{1 - e^{\varepsilon_0 \lambda/(1+\varepsilon_0)}}$$

where ε_0 is the initial ratio of active to inactive cells and λ is the initial mean number of cells per droplet. The enrichment (η) is defined as the ratio of ε after sorting (ε_1) to ε before sorting (ε_0) (ESI).†

The derivation of this model is fully described in the ESI† and a plot of η_m as a function of ε_0 and λ is shown in Fig. 6c. The observed value of η (η_{exp}) was predicted to match η_m and, therefore, increase with decreasing ε_0 or decreasing λ. It was not expected that η_{exp} would be significantly affected by sorting errors when η_m was less than 10^4 because of the low false positive error rate of the sorting device (<1 in 10^4 droplets).

To test the model, we performed a series of sorts with mixed populations of *lacZ* and Δ*lacZ* cells, where we varied both ε_0 (0.01–1) and λ (0.016–1.6). For each sort, ε_0 was verified and ε_1 was determined by plating-out cell suspensions on agar medium containing X-gal and counting blue (*lacZ*) and white (Δ*lacZ*) colonies (Fig. 6a and Table S1, ESI).† Bright-field microscopy was used to measure the proportion of droplets occupied by bacterial colonies and, by extension, λ. The results of the sorts are shown in Fig. 6b and compared to the theoretical enrichments in Fig. 6c. As predicted, η_{exp} was observed to increase with decreasing ε_0 or decreasing λ. At low λ (0.021 and 0.016), all the recovered cells were positive (*lacZ*). η_{exp} was found to be always within 5-fold of the predicted η_m value, suggesting that the model was accurate and that the Poisson distribution was indeed the dominant factor in determining enrichment. It is noteworthy that we also succeeded in recovering cells from a single sorted droplet (Fig. S3, ESI).†

Conclusions

We have demonstrated a highly efficient microfluidic sorting system that actively sorts droplets based on their fluorescence and used it to sort cells according to the presence or absence of an enzymatic activity. To allow more precise 'binning' of bacteria with specific activities, it would be necessary to eliminate membrane impermeability as a factor. For intracellular enzymes, such as β-galactosidase, this could be achieved by lyzing the cells while they are compartmentalized (Fig. S2, ESI);† alternatively, the enzyme could be secreted or displayed on the cell surface.

(a)

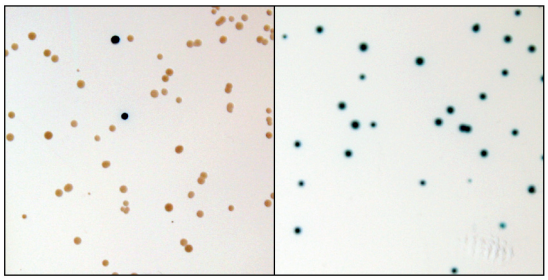

(b)

λ	ε_0	Number of droplets		ε_1	η_m	η_{exp}
		Analyzed	Sorted			
0.021	0.1	~4 × 10^4	10	>213	524	>2130
0.016	1	~1 × 10^5	100	>537	125	>537
0.16	0.01	~2 × 10^5	20	1.35	631	135
0.2	0.1	~6 × 10^4	100	7	55	70
0.15	1	~2 × 10^5	1000	16.1	14	16
1.6	0.01	~1 × 10^5	100	0.294	64	30
0.91	0.1	~2 × 10^5	1000	0.553	13	6

(c)

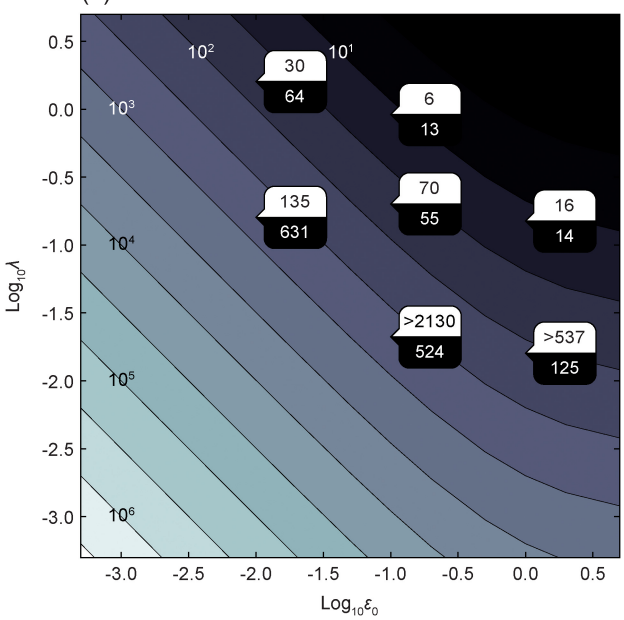

Fig. 6 Enrichment of cells by FADS based on β-galactosidase activity. (a) Photographs of *E. coli* colonies before (left photograph) and after sorting (right photograph) a $\varepsilon_0 \approx 0.1$, $\lambda \approx 0.01$ emulsion. The colonies grew on LB agar containing ampicillin, IPTG and X-gal for blue/white screening. The *lacZ* bacteria (blue colonies) were completely purified from the Δ*lacZ* bacteria (white colonies) during sorting, resulting in only *lacZ* colonies growing on the agar. (b) Predicted (η_m) and experimentally obtained (η_{exp}) enrichment values after one round of sorting as a function of λ and the starting ratio of active (*lacZ*) to inactive (Δ*lacZ*) cells (ε_0). For 7 combinations of λ and ε_0, sorts were performed and highly fluorescent (*lacZ*) droplets were collected. The initial (ε_0) and final (ε_1) values for ε were determined by blue/white colony screening. (c) A plot of the same data. A split box with a pointed projection at the relevant coordinates is shown for each combination of λ and ε_0. The relevant experimental value for η is shown (upper value; white background) along with the value predicted using the model (lower value; black background).

Indeed, FADS has already been used to sort *Bacillus subtilis* according to the activity of a secreted enzyme (Samuels *et al.*, unpublished) and to sort libraries of horseradish peroxidase displayed on *Sacharomyces cerevisiae* (Agresti *et al.*, unpublished). Beyond bacterial or yeast cells, FADS could be used to sort mammalian cells (which survive in droplets),[22,28] viruses or even single genes expressed *in vitro*.[23]

FADS has several other merits: setup time is short (<10 minutes per sample), reagent volumes are minimal (12 μl of aqueous phase generates 10^6 droplets), aerosols are not generated and very small numbers of cells (≥3000) can be handled (Fig. S3, ESI).† The inverse correlation observed between error rate and throughput suggests that the system can be operated in different modes (as in FACS). When a high λ is used, co-compartmentalization events are frequent (26.4% when $\lambda = 1$), so a false positive error rate of 1 in 100 droplets is acceptable and high throughputs can be used (~2000 droplets s^{-1} or ~2000 cells s^{-1}): sorting errors would not significantly affect enrichment until $\varepsilon_0 \leq 0.01$, at which point enrichment would plateau at ~100-fold (Fig. 6c). In contrast to this 'enrichment' mode, FADS can also be performed in 'purification' mode by using lower λ values and lower throughputs, thereby reducing error rates and allowing cells to be sorted to high purities. Theoretically, enrichment values at any speed could be improved by rejecting droplets containing co-compartmentalized negative cells while sorting (as in FACS) or by exploiting self-organizational behavior of cells during compartmentalization to eliminate the Poisson distribution itself.[29]

It is worth noting that by integrating the sorting device with modules for droplet splitting[12,15,16] and/or fusion[12–14] within the same chip, it should be possible to perform sophisticated assays involving high-speed manipulations that are currently impossible with existing technologies. Such tools would be enormously useful to fields such as directed evolution and proteomics.

Experimental

Materials

All materials were obtained from Sigma-Aldrich Co. unless otherwise stated.

Microfluidic devices

Each microfluidic device was prepared from poly-(dimethylsiloxane) (PDMS) by standard soft-lithography techniques.[30] A mould of SU-8 resist (MicroChem Corp.) was fabricated on a silicon wafer (Siltronix) by UV exposure (MJB3 contact mask aligner; SUSS MicroTec) through a photolithography mask (Fig. S1; Selba SA) and subsequent development (SU-8 developer; MicroChem Corp.). A curing agent was added to the PDMS base (Sylgard 184 silicone elastomer kit; Dow Corning Corporation) to a final concentration of 10% (w/w), mixed and poured over the mould to a depth of 5 mm. Following degassing for several minutes and cross-linking at 65 °C for several hours, the PDMS was peeled off the mould and the input and output ports were punched with a 0.75 mm-diameter Harris Uni-Core biopsy punch (Electron Microscopy Sciences). Particles of PDMS were cleared from the ports using pressurized nitrogen gas. The structured side of the PDMS slab was bonded

to a 76 × 26 × 1 mm glass microscope slide (Paul Marienfeld GmbH & Co. KG) by exposing both parts to an oxygen plasma (PlasmaPrep 2 plasma oven; GaLa Instrumente GmbH) and pressing them together. Finally, an additional hydrophobic surface coating was applied to the microfluidic channel walls by injecting the completed device with Aquapel glass treatment (PPG Industries) and then purging the liquid with nitrogen gas.

If necessary, electrodes were included in the microfluidic device as additional microfluidic channels, which were filled with metal: the device was heated to 85 °C and a 51In/32.5Bi/16.5Sn low-temperature solder (Indium Corporation) was melted inside the electrode channels.[31] Electrical connections with the solder electrodes were made with short pieces of electrical wire (Radiospares).

The FADS system itself was composed of several modules. Firstly, an emulsification device was used to generate the droplets by flow-focusing an aqueous stream with two streams of fluorinated oil containing a surfactant[11] (Fig. 1a). Emulsification devices for generating a single type of droplet ('single emulsifiers') (Fig. S1a, ESI)† were fabricated with a channel depth of 25 μm microns and devices for generating two emulsions simultaneously ('dual emulsifiers') (Fig. S1b, ESI)† were fabricated with a channel depth of 21 μm. Single emulsifiers were used to emulsify bacterial cells while dual emulsifiers were used to generate mixed emulsions for analyzing sorting efficiency. The second device was a droplet reservoir consisting of either a syringe (no gas-exchange) or an open-topped Pasteur pipette (for gas exchange) (Fig. 1b). The final module was a sorting device (Fig. S1c, ESI)† in which droplets were reloaded, spaced-out with fluorinated oil at a flow-focusing junction (Fig. 1c) and finally sorted at a Y-junction, triggering on droplet fluorescence (Fig. 1d). Sorting devices were fabricated with a channel depth of 21 μm.

Optical setup, data acquisition and control system

The optical setup (Fig. 2) consisted of an Axiovert 200 inverted microscope (Carl Zeiss SAS) mounted on a vibration-dampening platform (Thorlabs GmbH). A 20 mW, 488 nm solid-state laser (LAS; Newport-Spectraphysics) was mounted on the platform *via* a heatsink (Newport-Spectraphysics). The laser beam was shaped into a ~10 × ~150 μm line by a combination of a 25 mm-diameter cylindrical lens (effective focal length: −50 mm; Thorlabs GmbH) and a 25 mm-diameter plano-convex lens (effective focal length: 25 mm; Thorlabs GmbH) with a 5 cm distance between them (LL). The shaped beam was guided to the side camera port of the microscope *via* a series of periscope assemblies (Thorlabs GmbH). Inside the microscope, the laser light was reflected up into a LD Plan Neofluar 40×/0.6 microscope objective (OBJ; Carl Zeiss SAS) and focused across a channel within the microfluidic device (CHIP). A Phantom v4.2 high-speed digital camera (CAM; Vision Research) was mounted on the top camera port of the microscope to capture digital images during droplet production and sorting. A 488 nm notch filter (F1; Semrock Inc.) positioned in front of the camera protected the camera's sensor from reflected laser light. Light emitted from fluorescing droplets was captured by the objective and channeled back along the path of the laser into the system of periscope assemblies. The emitted light was separated from the laser beam by a 488/532/638 nm-wavelength transmitting dichroic beam splitter (DBS; Semrock Inc.), passed through a 510 nm bandpass filter (F2; 20 nm bandwidth; Semrock Inc.) and collected in an H5784-20 photomultiplier tube (PMT; Hamamatsu Photonics KK). Data acquisition (DAQ) and control was performed by a PCI-7831R Multifunction Intelligent DAQ card (National Instruments Corporation) executing a program written in LabView 8.2 (National Instruments Corporation). The data acquisition rate for the system was 100 kHz. To sort a particular droplet, the DAQ card provided a signal to a Model 623B high-voltage amplifier (Trek Inc.), connected to the electrodes of the microfluidic device. Liquids were pumped into the microfluidic device using standard-pressure infusion-only PHD 22/2000 syringe pumps (Harvard Apparatus Inc.). Syringes were connected to the microfluidic device using 0.6 × 25 mm Neolus needles (Terumo Corporation) and PTFE tubing with an internal diameter of 0.56 mm and an external diameter of 1.07 mm (Fisher Bioblock Scientific).

Factors affecting sorting

A solution of 250 μM sodium fluorescein was prepared in a 50 mM Tris-HCl buffer pH 7. The solution was loaded into an Omnifix-F 1 ml disposable syringe (B. Braun Medical AG) and pumped into a single-emulsifier microfluidic device (Fig. S1a, ESI)† at a rate of 200 μl h^{-1}. The fluorinated oil FC-40 (3M), containing 2.5% (w/w) Krytox-DMP surfactant,[22] was pumped into the device from a 5 ml Injekt disposable syringe (B. Braun Medical AG) at a rate of 1 ml h^{-1}. The stream of fluorescein was flow-focused between two streams of fluorinated oil/surfactant mixture, yielding droplets of 12 pl (28 μm in diameter when spherical) at a rate of ~4000 droplets s^{-1} (Movie S1, ESI).† Approximately 500 μl of emulsion were collected in an Omnifix-F 1 ml syringe with its plunger in place.

Next, the collected droplets were injected into the sorting device (Fig. S1c, ESI),† spaced-out with surfactant-free fluorinated oil (Movie S2, ESI)† and analyzed by the optical setup as they flowed into the sorting junction. Individual droplets were sorted by applying a square-wave pulse to the high-voltage amplifier, which amplified the voltage 1000-fold.

The following factors were observed to affect sorting: Q_{em}, the flow rate of the reinjected emulsion; Q_{flu}, the flow rate of the fluorinated oil for spacing-out the droplets; τ_{sort}, the duration of the sorting pulse; and U_{sort}, the peak-to-peak voltage applied across the electrodes.

Measurement of sorting efficiency

Image analysis was used to accurately define the error rates of the device when sorting droplets at the throughput chosen for sorting cells (300 droplets s^{-1}).

Two solutions of sodium fluorescein were prepared in a 50 mM Tris-HCl buffer pH 7: 25 and 100 μM. 12 pl droplets of each solution were generated simultaneously using a dual-emulsifier microfluidic device (Fig. S1b, ESI).†

The droplets in the mixed emulsion were injected into the device (300 droplet s^{-1}) and sorted as a function of fluorescence to select only those droplets containing 100 μM sodium fluorescein. The parameters for sorting were: Q_{em} = 15–50 μl h^{-1},

$Q_{flu} = 0.8–1.2$ ml h^{-1}, F (the frequency of the sorting pulse) = 30 kHz, $\tau_{sort} = 0.4–1$ ms and $U_{sort} = 1–1.4$ $kV_{p\text{-}p}$. These parameters were fine-tuned before each sort to ensure that droplets were correctly sorted and that no droplets flowed down the 'positive' arm of the sorting junction when the electric field was not applied. This fine-tuning was required because of slight variations in channel depth between devices, the distance of the electrodes from the sorting channel, the average droplet volume in the emulsion and unintended variations in the pumping rates from the syringe pumps.

The high-speed camera was triggered after sorting each droplet, allowing the operator to ensure that sorted droplets were being directed down the correct arm of the sorting junction. $\Delta\tau_{cam}$, the delay between the falling edge of the peak in fluorescence and the trigger pulse sent to the high-speed camera, was ~800 μs.

To determine the efficiency of sorting a MATLAB script (The MathWorks Inc.) was used to analyze individual frames from the high-speed camera. The principle of the analysis was to first determine the light intensity of the laser line as a droplet flowed past: this intensity correlated with the concentration of fluorescein in the droplet. Subsequent frames followed the trajectory of the droplet through the sorting junction as it was either sorted or not. By measuring the pixel intensities in each arm of the sorter, it was possible to determine whether the droplet ended up in the correct arm of the sorter. This method enabled us to analyze the sorting of $\sim 10^4$ droplets.

E. coli strains and preparation of cell suspensions

Standard molecular biology protocols were used to transform *E. coli* T7 Express cells (New England Biolabs Inc.) with the plasmids pIVEX2.2EM-*lacZ* (encoding β-galactosidase) and pIVEX2.2EM-Δ*lacZ* (encoding a frameshifted, inactive mutant of β-galactosidase).[9] 5 ml aliquots of LB containing 100 μg ml^{-1} ampicillin were inoculated with single colonies of the resulting strains. These aliquots were grown for 14 hours at 37 °C with a 230 rpm shaking. The following day, fresh 5 ml aliquots of LB containing ampicillin were inoculated with 50 μl of each overnight culture and grown under the same conditions to mid-log phase (an OD_{600} of 0.3–0.4). The growing cultures were rediluted 100-fold into LB containing ampicillin and 1 mM isopropyl β-D-1-thiogalactopyranoside (IPTG) to induce expression of either β-galactosidase or the inactive variant. After 3 hours, the cells in each induction culture were harvested (at an OD_{600} of 0.5–0.6) by centrifuging at 3000 × *g* for 5 minutes at 4 °C. The supernatant was removed and the cell pellet was resuspended with 5 ml of ice-cold LB containing ampicillin. This washing step was repeated two further times to remove free enzyme from the cultures and, thus, lower the amount of background activity. The optical density of each resuspended culture was adjusted to an OD_{600} of 0.45. The cell suspensions were mixed together in the appropriate ratio for each experiment and diluted if necessary. The ratio was confirmed for each experiment by diluting an aliquot of the suspension to an OD_{600} of 4.5×10^{-5} and plating 50–100 μl on an imMedia Blue Amp agar plate (Invitrogen Corporation), containing ampicillin, IPTG and 5-bromo-4-chloro-3-indolyl-β-D-galactopyranoside (X-gal). Plates were incubated at 37 °C for 14 hours, 4 °C for 24 hours (to develop the color of the blue colonies) and digitally imaged.

Emulsification of cell suspensions on-chip

Each cell suspension was emulsified in HFE-7500 fluorinated oil (3M, St. Paul, Minnesota, USA) containing 2% (w/w) EA surfactant (RainDance Technologies, Lexington, MA, USA), which is a PEG–PFPE amphiphilic block copolymer.[32] The cell suspension was loaded into a 250 μl gas-tight syringe (Hamilton Company) and pumped into the emulsification device (Fig. S1a, ESI)† at a rate of 100 μl h^{-1}. A solution of LB containing ampicillin, 100 μM FDG (Euromedex) and 1 μM sodium fluorescein, was loaded into another syringe and pumped in at the same rate. These streams combined just before the nozzle of the device and were flow-focused by two streams of the fluorinated oil/surfactant mixture flowing at 1–1.15 ml h^{-1} from a 1 ml gas-tight syringe. The aqueous stream broke up into a series of 12 pl droplets at a rate of ~4600 droplets s^{-1}. The generated emulsion flowed off-chip through a 20 cm-length of Intramedic poly(ethylene terephthalate) (PET) PE 20 tubing (Becton, Dickinson and Company) to a glass Pasteur pipette containing 100 μl of LB with ampicillin (Fig. 1b). The emulsion was collected underneath the less-dense LB for 12 minutes, yielding a total volume of 40 μl. The PET tubing was sealed and the pipette was incubated at 20 °C for 12 hours. The layer of LB above the emulsion was necessary to prevent evaporation and coalescence, but still allow gas exchange with the atmosphere. Gas exchange was essential for the proliferation of cells in each droplet and the subsequent detection of β-galactosidase activity.

λ was determined for each emulsion following incubation by bright-field microscopy. The cells inside occupied droplets proliferated into small clonal populations ('colonies') overnight, which could be counted (Movie S6, ESI).† λ was found using the equation:

$$\lambda = -\ln(1 - k)$$

where k is the fraction of droplets occupied by colonies.

Sorting cells in droplets based on enzymatic activity

Excess fluorinated oil beneath the emulsion was drained and discarded. A 40 cm-length of Intramedic PET tubing was connected with a 0.4 × 16 mm Neolus needle (Terumo Corporation) to a Omnifix-F 1 ml syringe previously filled with ddH_2O. The tubing was primed with the ddH_2O and connected to the Pasteur pipette using a PDMS connector block. A standard-pressure infuse/withdraw PHD 22/2000 syringe pump (Harvard Apparatus Inc.) was used to displace the plunger in the syringe and load the emulsion into the tubing at a rate of 200 μl h^{-1}. After loading, the direction of flow was reversed and adjusted to 100 μl h^{-1}. The tubing was connected to the sorting device (Fig. S1c, ESI).† Surfactant-free fluorinated oil was pumped into the device at a rate of 1 ml h^{-1} to space out the droplets in the sorting channel. When the system had stabilized, the flow rate of the reinjected emulsion was reduced to 20 μl h^{-1}. The droplets were analyzed by the optical setup and highly fluorescent droplets were sorted (Movie S5, ESI).†Sorted droplets were collected in a 'collection loop' consisting of a coiled 25 cm length of PTFE tubing. Owing to the lower density of the droplets compared to the surrounding fluorinated oil, the droplets accumulated at the highest point in the loop. It was possible to trap even single droplets by this approach (Fig. S3, ESI).†

Recovery of cells from sorted droplets

Following a sort, droplets were recovered from the collection loop by sealing the end of the loop, severing it at about 2 cm distance from the chip and draining it into a 1.5 ml microcentrifuge tube (Axygen Inc.). To dislodge any droplets remaining in the loop, it was flushed with a 30 μl plug of Droplet Destabilizer (RainDance Technologies, Lexington, MA, USA) followed by 200 μl of LB containing ampicillin (using a syringe). The emulsion was completely broken by vortexing the microcentrifuge tube in a vigorous manner for 30 s. The broken emulsion was then briefly centrifuged (1000 × *g* for 3 s) and 150 μl of the supernatant—consisting of LB and *E. coli* cells in suspension—were transferred to a new microcentrifuge tube. A fraction of this suspension was plated on imMedia Amp Blue agar plates, equivalent to 10 droplets (resulting in ~500 colonies). This procedure was not modified when recovering single droplets.

Acknowledgements

J.-C. B. was supported by a European Molecular Biology Organization long-term fellowship. O. J. M. was supported by the Medical Research Council (UK), the Ministry of Defence (UK) and the Human Frontier Science Program (HFSP). AE-H was supported by the European Commission Framework Programme 6 (EC FP6) MiFem Network. L. F. was supported by the EC FP6 Marie Curie Research Training Network, ProSA. J. J. A. and D. A. W. were supported by the NSF (DMR-0602684 and DBI-0649865) and the Harvard MRSEC (DMR-0820484). This work was also supported by the Ministère de l'Enseignement Supérieur et de la Recherche, Centre National de la Recherche Scientifique (CNRS), Agence National de la Recherche (ANR) (ANR-05-BLAN-0397) and the Fondation d'entreprise EADS.

References

1 L. M. Mayr and P. Fuerst, The future of high-throughput screening, *J. Biomol. Screen.*, 2008, **13**, 443–448.
2 M. Eisenstein, Cell sorting: divide and conquer, *Nature*, 2006, **441**, 1179–1185.
3 H. M. Shapiro, *Practical flow cytometry*. Wiley–Liss, New York, 2003.
4 I. Schmid, C. Lambert, D. Ambrozak, G. E. Marti, D. M. Moss and S. P. Perfetto, International society for analytical cytology biosafety standard for sorting of unfixed cells, *Cytometry A*, 2007, **7**, 414–437.
5 V. Kiermer, FACS-on-a-chip, *Nat. Methods*, 2005, **2**, 91.
6 T. D. Perroud, J. N. Kaiser, J. C. Sy, T. W. Lane, C. S. Branda, A. K. Singh and K. D. Patel, Microfluidic-based cell sorting of Francisella tularensis infected macrophages using optical forces, *Anal. Chem.*, 2008, **80**, 6365–6372.
7 D. S. Tawfik and A. D. Griffiths, Man-made cell-like compartments for molecular evolution, *Nat. Biotechnol.*, 1998, **16**, 652–656.
8 A. Aharoni, G. Amitai, K. Bernath, S. Magdassi and D. S. Tawfik, High-throughput screening of enzyme libraries: thiolactonases evolved by fluorescence-activated sorting of single cells in emulsion compartments, *Chem. Biol.*, 2005, **12**, 1281–1289.
9 E. Mastrobattista, V. Taly, E. Chanudet, P. Treacy, B. T. Kelly and A. D. Griffiths, High-throughput screening of enzyme libraries: in vitro evolution of a beta-galactosidase by fluorescence-activated sorting of double emulsions, *Chem. Biol.*, 2005, **12**, 1291–1300.
10 A. D. Griffiths and D. S. Tawfik, Miniaturising the laboratory in emulsion droplets, *Trends Biotechnol.*, 2006, **24**, 395–402.
11 S. Anna, N. Bontoux and H. Stone, Formation of dispersions using "flow focusing" in microchannels, *Appl. Phys. Lett.*, 2003, **82**, 364–366.
12 H. Song, J. Tice and R. Ismagilov, A microfluidic system for controlling reaction networks in time, *Angew. Chem., Int. Ed.*, 2003, **42**, 768–772.
13 K. Ahn, J. Agresti, H. Chong, M. Marquez and D. Weitz, Electrocoalescence of drops synchronized by size-dependent flow in microfluidic channels, *Appl. Phys. Lett.*, 2006, **88**, 264105.
14 C. Priest, S. Herminghaus and R. Seemann, Controlled electrocoalescence in microfluidics: Targeting a single lamella, *Appl. Phys. Lett.*, 2006, **89**, 134101.
15 D. Link, S. Anna, D. Weitz and H. Stone, Geometrically mediated breakup of drops in microfluidic devices, *Phys. Rev. Lett.*, 2004, **92**, 054503.
16 L. Ménétrier-Deremble and P. Tabeling, Droplet breakup in microfluidic junctions of arbitrary angles, *Phys. Rev. E Stat. Nonlin. Soft Matter Phys*, 2006, **74**, 035303.
17 D. R. Link, E. Grasland-Mongrain, A. Duri, F. Sarrazin, Z. Cheng, G. Cristobal, M. Marquez and D. A. Weitz, Electric control of droplets in microfluidic devices, *Angew. Chem., Int. Ed.*, 2006, **45**, 2556–2560.
18 K. Ahn, C. Kerbage, T. Hunt, R. Westervelt, D. Link and D. Weitz, Dielectrophoretic manipulation of drops for high-speed microfluidic sorting devices, *Appl. Phys. Lett.*, 2006, **88**, 024104.
19 L. M. Fidalgo, G. Whyte, D. Bratton, C. F. Kaminski, F. Clemens, C. Abell and W. T. S. Huck, From microdroplets to microfluidics: selective emulsion separation in microfluidic devices, *Angew. Chem., Int. Ed.*, 2008, **47**, 2042–2045.
20 C. N. Baroud, J.-P. Delville, F. Gallaire and R. Wunenburger, Thermocapillaryvalve for droplet production and sorting, *Phys. Rev. E Stat. Nonlin. Soft Matter Phys*, 2007, **75**, 046302.
21 M. Chabert and J.-L. Viovy, Microfluidic high-throughput encapsulation and hydrodynamic self-sorting of single cells, *Proc. Natl. Acad. Sci. U. S. A.*, 2008, **105**, 3191–3196.
22 J. Clausell-Tormos, D. Lieber, J. C. Baret, A. El-Harrak, O. J. Miller, L. Frenz, J. Blouwolff, K. J. Humphry, S. Köster, H. Duan, C. Holtze, D. A. Weitz, A. D. Griffiths and C. A. Merten, Droplet-based microfluidic platforms for the encapsulation and screening of mammalian cells and multicellular organisms, *Chem. Biol.*, 2008, **15**, 427–437.
23 F. Courtois, L. F. Olguin, G. Whyte, D. Bratton, W. T. S. Huck, C. Abell and F. Hollfelder, An integrated device for monitoring time-dependent in vitro expression from single genes in picolitre droplets, *Chembiochem.*, 2008, **9**, 439–446.
24 A. Huebner, M. Srisa-Art, D. Holt, C. Abell, F. Hollfelder, A. J. deMello and J. B. Edel, Quantitative detection of protein expression in single cells using droplet microfluidics, *Chem. Commun.*, 2007, 1218–1220.
25 R. Nir, Y. Yisraeli, R. Lamed and E. Sahar, Flow cytometry sorting of viable bacteria and yeasts according to beta-galactosidase activity, *Appl. Environ. Microbiol.*, 1990, **56**, 3861–3866.
26 D. R. Storm, K. S. Rosenthal and P. E. Swanson, Polymyxin and related peptide antibiotics, *Annu. Rev. Biochem.*, 1977, **46**, 723–763.
27 R. G. Ashcroft and P. A. Lopez, Commercial high speed machines open new opportunities in high throughput flow cytometry (htfc), *J. Immunol. Methods*, 2000, **243**, 13–24.
28 S. Köster, F. E. Angilè, H. Duan, J. J. Agresti, A. Wintner, C. Schmitz, A. C. Rowat, C. A. Merten, D. Pisignano, A. D. Griffiths and D. A. Weitz, Drop-based microfluidic devices for encapsulation of single cells, *Lab Chip*, 2008, **8**, 1110–1115.
29 J. F. Edd, D. Di Carlo, K. J. Humphry, S. Köster, D. Irimia, D. A. Weitz and M. Toner, Controlled encapsulation of single-cells into monodisperse picolitre drops, *Lab Chip*, 2008, **8**, 1262–1264.
30 D. C. Duffy, J. C. McDonald, O. J. A. Schueller and G. M. Whitesides, Rapid prototyping of microfluidic systems in poly(dimethylsiloxane), *Anal. Chem.*, 1998, **70**, 4974–4984.
31 A. C. Siegel, D. A. Bruzewicz, D. B. Weibel and G. M. Whitesides, Microsolidics: Fabrication of three-dimensional metallic microstructures in poly(dimethylsiloxane), *Adv. Mater.*, 2007, **19**, 727–733.
32 C. Holtze, A. C. Rowat, J. J. Agresti, J. B. Hutchison, F. E. Angilè, C. H. J. Schmitz, S. Köster, H. Duan, K. J. Humphry, R. A. Scanga, J. S. Johnson, D. Pisignano and D. A. Weitz, Biocompatible surfactants for water-in-fluorocarbon emulsions, *Lab Chip*, 2008, **8**, 1632–1639.

